ACS Medicinal Chemistry Letters

pubs.acs.org/acsmedchemlett

Letter

Hydrophobic Tagging-Induced Degradation of PDEδ in Colon Cancer Cells

Menglu Guo,[†] Shipeng He,[†] Junfei Cheng, Yu Li, Guoqiang Dong,* and Chunquan Sheng*

Cite This: *ACS Med. Chem. Lett.* 2022, 13, 298−303

Read Online

ACCESS | Metrics & More | Article Recommendations | Supporting Information

ABSTRACT: The development of KRAS−PDEδ protein−protein interaction (PPI) inhibitors is generally hampered by limited antitumor activity. Herein, the first hydrophobic tagging (HyT)-based PDEδ degraders were designed. Compound **17c** efficiently bound to PDEδ and induced degradation of PDEδ in SW480 colon cancer cells. As compared with PDEδ inhibitor deltazinone, HyT-based degrader **17c** exhibited improved antitumor activity toward KRAS mutant cancer cells. This study highlighted the potential of HyT as a valuable chemical tool for tumorigenic PDEδ knockdown, which could be developed into a promising strategy for antitumor drug discovery.

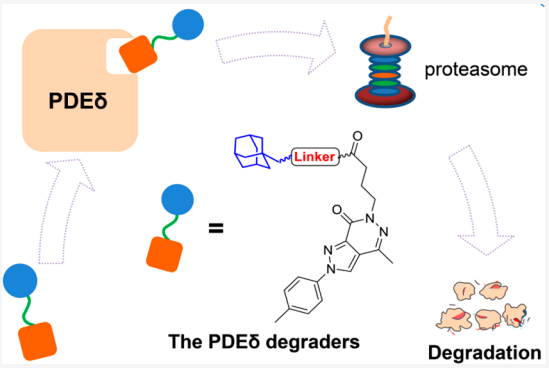

KEYWORDS: *KRAS−PDEδ PPI, HyT, PDEδ degrader, antitumor*

Kirsten rat sarcoma 2 viral oncogene homologue (KRAS) protein is closely related to the occurrence and development of tumors.[1−3] Notably, almost 86% of pancreatic cancers and 41% of colon cancers are associated with KRAS mutations. After translation, KRAS protein is modified in the C-terminal hypervariable region and then transported to the cell membrane, executing the function that binds it with the related effector proteins to activate the downstream signaling pathway.[4,5] In cancer cells, the conformation of KRAS is changed and the KRAS mutants continue to bind with GTP to produce abnormal proliferation signals, resulting in the continuous proliferation of tumor cells. Therefore, KRAS and related signaling pathways were regarded as important targets for the development of antitumor therapeutics.[6−9]

KRAS−PDEδ protein−protein interaction (PPI) plays an important role in the functional regulation of KRAS.[10] PDEδ regulates the localization of KRAS on the cell membrane.[11] The hydrophobic cavity of PDEδ binds to the farnesylated KRAS, which enhances the dissolution and diffusion of KRAS in the cells and promotes the correct localization and enrichment of KRAS in the cytoplasm. The inhibition of PDEδ leads to abnormal transport and distribution of KRAS, thus interfering with KRAS signal transduction pathway and inhibiting proliferation of tumor cells.[11−13]

In recent years, a number of small molecule KRAS−PDEδ inhibitors (Figure 1), such as deltazinone (**1**),[14−16] deltarasin (**2**),[9,17] and deltasonamide (**3**),[18] have been reported. We also discovered several classes of small molecule PDEδ inhibitors (**4**−**6**) through structure-based drug design.[19,20] These inhibitors generally exhibited potent PDEδ binding activity and effectively blocked the KRAS−PDEδ PPI. However, most of them are limited by poor antitumor activity, because endogenous Arl2 could induce the fast release of inhibitors from PDEδ.[18] Thus, novel modulation strategies are highly desirable to block the KRAS−PDEδ PPI.

Hydrophobic tagging (HyT) has emerged as a promising strategy for targeted protein degradation through ubiquitination-proteasome system.[21,22] The HyT approach induces a hydrophobic and bulky group (e.g., amantadine) to a small-molecule ligand of the target protein. The hydrophobic group of HyT is located on the surface of the target protein, which is regarded as a misfolded part (a partially unfolded protein) by the protein repair mechanism. The "unfolded" protein would then be folded by the chaperone protein. However, after failing to repeat folding, the target protein will be recognized and degraded by the ubiquitin-proteasome system to maintain the homeostasis of cell function (Figure 2A). As an alternative strategy of PROTACs[23] (proteolysis targeting chimeras), the HyT technology has been successfully used to degrade various drug targets, such as HaloTag fusion proteins,[24] erythroblastosis oncogene B3 (ERBB3),[25] and androgen receptor (AR).[26]

Received: November 30, 2021
Accepted: January 10, 2022
Published: January 12, 2022

https://doi.org/10.1021/acsmedchemlett.1c00670
ACS Med. Chem. Lett. 2022, 13, 298−303

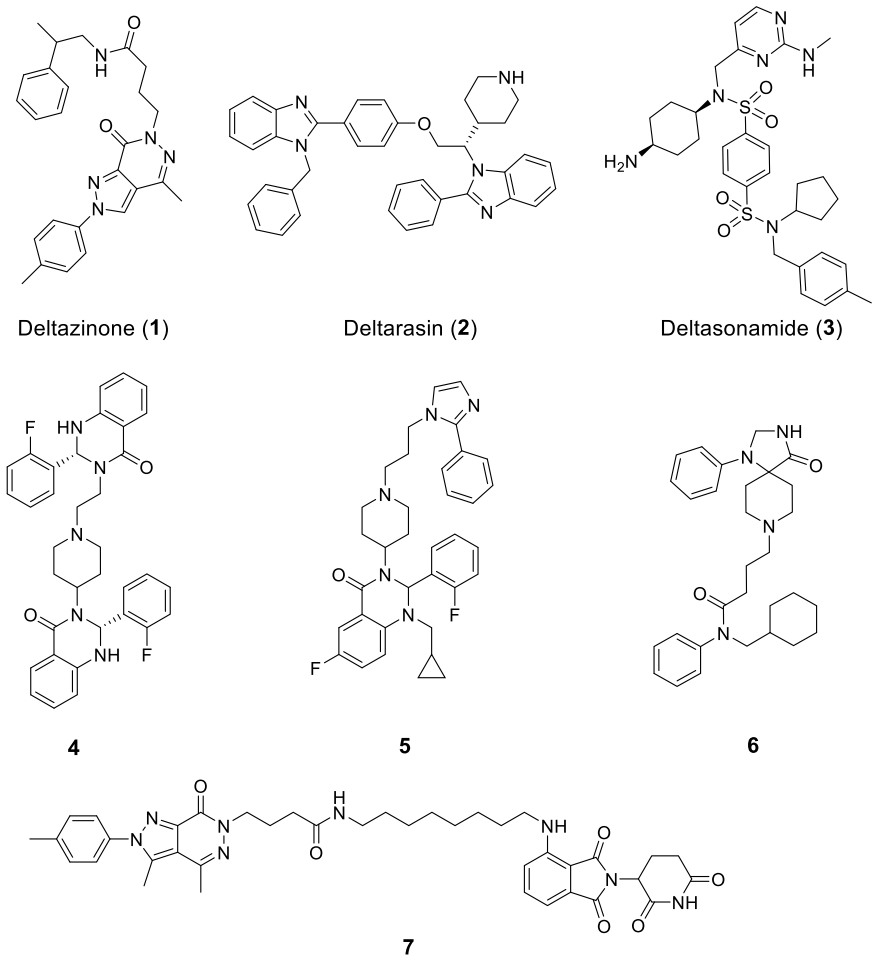

Figure 1. Representative KRAS−PDEδ PPI inhibitors and degraders

However, as compared with PROTACs, the successful examples of HyT-based degraders are rather limited.

Previously, we confirmed that targeted protein degradation was an effective strategy to interfere with the function of KRAS-PDEδ interaction and designed the first PDEδ degrader (**7**) using the PROTAC approach.[27] Herein we designed the first HyT-mediated PDEδ degraders, which showed potent PDEδ degrading potency and antitumor activity.

Deltazinone (compound **1**) is a highly potent small molecule KRAS−PDEδ inhibitor, which has been widely used as a lead compound or tool molecule in the studies of KRAS−PDEδ PPI.[14] Starting from compound **1**, we have successfully designed potent inhibitors and PROTAC-based degraders of PDEδ. Inspired by these results, herein, compound **1** was selected as a template molecule for the design of HyT-based degraders. The predicted binding model of compound **1** with PDEδ indicates that the terminal phenylamine is exposed to the protein surface (Figure 2B), offering a favorable site for inducing HyT groups. Moreover, structural modification of terminal phenylamine had little effect on the binding affinity with PDEδ. For example, replacement of the phenylamine group of compound **1** with amphetamine was tolerated (compound **8**).[14] Therefore, the terminal phenyl group was replaced by a linker and a HyT group (amantadine), resulting in a series of new PDEδ degraders (Figure 2C, compounds **15**−**17**). Theoretically, the amantadine HyT could simulate the misfolding of the PDEδ protein and the unfolded protein is recognized and degraded by ubiquitin-proteasome system, thus blocking the KRAS-PDEδ PPI.

The procedures for the synthesis of target compounds were outlined in Schemes S1−S4. Commercially available 4-methylaniline (**9**) was transformed to compound **10** through diazotization and a coupling reaction. Following the cyclization reaction of compound **10**, intermediate **11** was obtained, which was further cyclized to afford intermediate **12** under the conditions of hydrazine hydrate in EtOH. Compound **12** was reacted with methyl 4-bromobutanoate via a nucleophilic substitution reaction to give intermediate **13**, which was subsequently subjected to ester hydrolysis reaction to afford the corresponding carboxylic acid **14**. Target compounds **15a** and **15b** were prepared by condensing key intermediate **14** with amantadine and 1-adamantanemethylamine, respectively (Scheme S1). An amidation reaction between commercially available starting material **18** and different Boc-*N*-carboxylic acids obtained compounds **19a** and **19b**. The Boc group of intermediates **19a** and **19b** were deprotected to give compounds **16a** and **16b**, which were further condensed with intermediate **14** to yield compounds **16a** and **16b**. Compound **18** and various dicarboxylic monomethyl esters were reacted to afford compounds **21a**−**21c**, which were further hydrolyzed and condensed with *tert*-butyl 4-aminophenethylcarbamate to afford intermediates **23a**−**23c**. After deprotection, compounds **24a**−**24c** were condensed with intermediate **14** in the presence of HATU and DIPEA to give target compounds **16c**−**16e** (Scheme S2). Commercially available reagents **25a**−**25e** were condensed with compound **14** to yield corresponding intermediates, which were subsequently deprotected to obtain

https://doi.org/10.1021/acsmedchemlett.1c00670
ACS Med. Chem. Lett. 2022, 13, 298−303

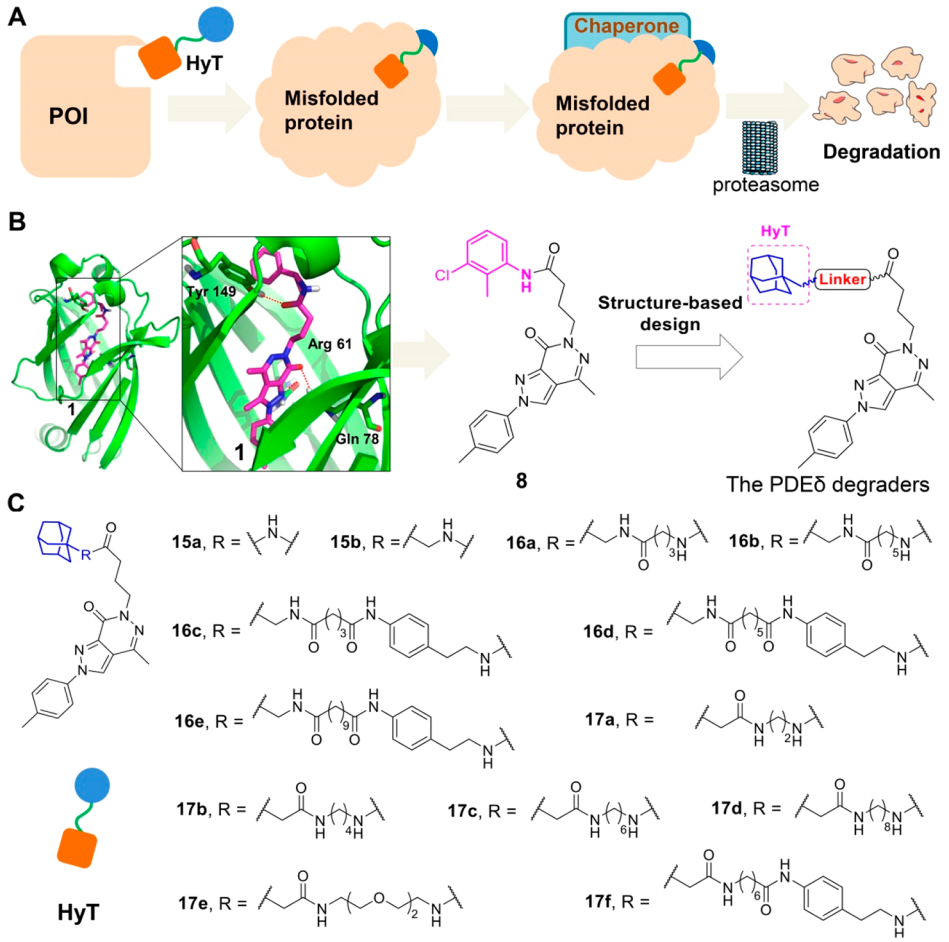

Figure 2. HyT-mediated degraders of PDEδ. (A) Schematic diagram of the HyT technology. (B) Rational design of HyT-based PDEδ degraders by the prediction of binding model of compound **1** with PDEδ (PDB code 5E80). (C) Structure of target compounds **15a**−**17f**.

Table 1. PDEδ Binding Affinity and Antiproliferative Activities of Target Compounds[a]

compds	linker	K_i (nM)	IC_{50} (μM)	
			SW480	HCT116
15a	$n = 0$	13.6 ± 9.4	>100	>100
15b	CH_2	9.3 ± 1.7	>100	>100
16a	$(CH2)_3$	41.0 ± 18.0	8.0 ± 1.2	11.4 ± 1.6
16b	$(CH_2)_5$	44.4 ± 6.8	>100	32.5 ± 7.5
16c	$(CH_2)_3$	8.6 ± 1.3	19.8 ± 12.7	39.0 ± 1.5
16d	$(CH_2)_5$	45 ± 10.2	>100	>100
16e	$(CH_2)_9$	>1000	14.0 ± 9.2	>100
17a	$(CH_2)_2$	38.8 ± 1.5	10.0 ± 5.5	20.4 ± 8.7
17b	$(CH_2)_4$	49.3 ± 13.0	7.0 ± 1.3	50.7 ± 0.1
17c	$(CH_2)_6$	26.0 ± 2.6	4.8 ± 0.2	7.7 ± 2.0
17d	$(CH_2)_8$	29.0 ± 0.7	5.6 ± 2.9	17.7 ± 3.2
17e	$CH_2(CH_2OCH_2)_2CH_2$	132.0 ± 5.1	5.4 ± 0.9	18.5 ± 5.8
17f	$(CH_2)_6$	146.5 ± 16.1	>100	>100
deltazinone (**1**)		8.0 ± 0.5	18.3 ± 8.3	82.4 ± 6.4

[a]Values represent a mean ± SD of at least three independent experiments. The values of K_i were obtained according to eqs S1−S6 in the Supporting Information.

compounds **26a**−**26e**. Target compounds **17a**−**17e** were afforded by reacting compounds **26a**−**26e** with 1-adamantane-acetic acid under the condition of HBTU and DIPEA (Scheme S3). Similar to the protocols for the synthesis of intermediates **26a**−**26e**, compound **29** was obtained via the condensation and hydrolysis reactions. Intermediate **29** was reacted with *tert*-butyl 4-aminophenethylcarbamate to afford compound **30**, which was deprotected to afford compound **31**. Finally, condensation between compound **31** and intermediate **14** yielded target compound **17f** (Scheme S4).

Initially, a fluorescence polarization (FP) binding assay was performed to investigate the binding affinity of all target

https://doi.org/10.1021/acsmedchemlett.1c00670
ACS Med. Chem. Lett. 2022, 13, 298−303

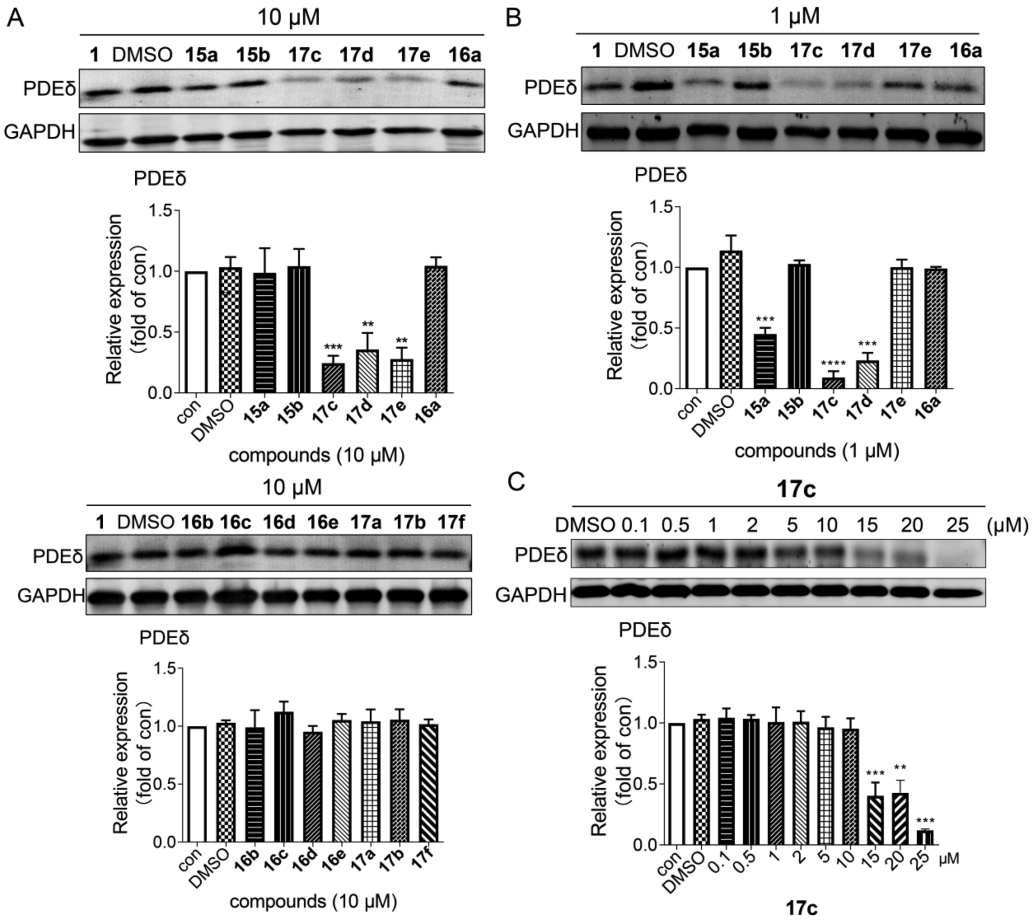

Figure 3. Effects of target compounds on the degradation of PDEδ. (A, B) Target compounds induced the degradation of PDEδ at 10 μM and 1 μM. (C) Compound **17c** dose-dependently degraded PDEδ. The protein expression contents of PDEδ were quantified by *ImageJ*. The data were confirmed at least three times (**P < 0.05 and ***P < 0.005 relative to the control group at indicated times).

compounds with PDEδ using compound **1** as the positive control. As shown in Table 1, most of the target compounds exhibited good binding activity. Compound **15a** with a short linker showed excellent PDEδ binding affinity (K_i = 13.6 nM). Compound **15b** with the linker extension of one carbon atom exhibited slightly enhanced PDEδ binding activity (K_i = 9.3 nM) to improve the flexibility of the terminal amantadine hydrophobic group. Subsequently, compounds containing various linkers were further synthesized and evaluated. However, with an increase in the alkyl linker length, the binding activity of compounds **16a** and **16b** were reduced to 41 and 44.1 nM, respectively. Compounds **16c**−**16e** were designed by introduction of the phenyl group to enhance the rigidity of the linker. However, their binding affinities were significantly decreased. These results demonstrated that the long alkyl linker might be unfavorable for PDEδ binding. Finally, the terminal amide group was reversed to obtain compounds **17a**−**17f**. Among them, two compounds, **17c** and **17d**, exhibited excellent binding activity, with K_i values of 26 and 29 nM, respectively.

In consideration of the binding activities, all the target compounds were further evaluated for the effects on PDEδ degradation in the SW480 cell line (KRAS mutant human colon cancer cells) by the Western blot analysis. As shown in Figure 3A, compounds **15a**, **16a**, and **17c**−**17e** significantly induced PDEδ degradation in SW480 cells at a concentration of 10 μM. Particularly, compound **17c** exhibited the best degrading activity (about an 86% degradation rate at 10 μM). However, no significant degradation was observed when the SW480 cells were treated with the other compounds. When the concentration was reduced to 1 μM (Figure 3B), compounds **15a**, **16a**, and **17c-d** retained the degradation activity. Among them, compound **17c** still achieved the best degradation activity (about 79% degradation rate at 1 μM). Furthermore, the dose-dependent effect of compound **17c** was explored (Figure 3C). The results indicated that compound **17c** exhibited significant PDEδ degradation in a concentration-dependent manner and achieved a DC_{50} (concentration causing 50% protein degradation) value of 11.4 μM in SW480 cells for 24 h. Next, the downstream proteins regulated by PDEδ were investigated (Figure 4A, B). Consistent with the positive drug, compound **17c** could downregulate p-Akt and p-Erk in a concentration-dependent manner, whereas it had little effect on the expression of t-Akt and t-Erk. These results suggested that compound **17c** effectively degraded PDEδ in SW480 cancer cells and then caused the changes in the downstream pathways.

Given the potent PDEδ binding activity and degradation efficiency, the antiproliferative activities of the target compounds were investigated against two different KRAS mutant human colon cancer cells (SW480 and HCT116 cell lines) by a cell counting kit-8 (CCK8) assay (Table 1). The results revealed that most of the target compounds showed better antiproliferative activity toward SW480 cells than that of HCT116 cells. As compared with the PDEδ inhibitor deltazinone, improved antitumor activities were observed for several HyT-based

https://doi.org/10.1021/acsmedchemlett.1c00670
ACS Med. Chem. Lett. 2022, 13, 298−303

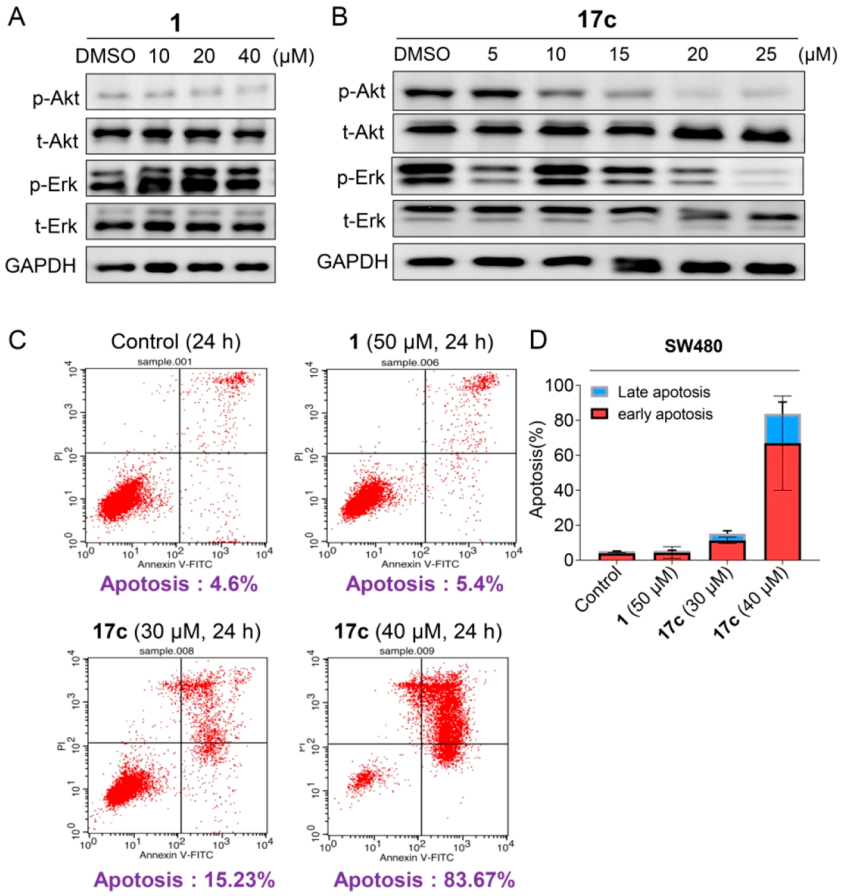

Figure 4. Antitumor mechanism of compound **17c.** (A, B) Change in PDEδ downstream proteins in SW480 cancer cells induced by compound **1** and compound **17c** for 24 h. The Western blot analysis was repeated at least three times. (C, D) Compound **17c** induced apoptosis of SW480 cancer cells after 24 h of treatment. All bar graphs present the mean ± SD.

degraders (e.g., compounds **16a**, **16e**, and **17a**−**17e**). Particularly, compound **17c** (SW480 IC_{50} = 4.8 μM; HCT116 IC_{50} = 7.7 μM) exhibited the best antiproliferative activity. Importantly, the in vitro antitumor efficacies of compounds **17c** were generally consistent with the degradation efficiency and the binding activity of PDEδ. Moreover, its antiproliferative activity was further evaluated against MIAPACA-2 pancreatic cancer cells (Figure S1). The results indicated that the IC_{50} value of compound **17c** was 17.5 μM, which was also significantly better than that of deltazinone (IC_{50} = 70.6 μM). Furthermore, the assay of flow cytometry with Annexin V/PI staining was performed to elucidate the antitumor mechanism of action of compound **17c**. As shown in panels C and D in Figure 4, compound **17c** significantly induced apoptosis of SW480 cells after 24 h of treatment. At a concentration of 40 μM, the apoptosis rate of compound **17c** was 83.67%, which was better than that of deltazinone (5.4% apoptosis rate at 50 μM). However, the definite correlation between degradation activity and apoptosis rate could not be detected at the experimental concentrations. Taken together, compound **17c**, the most potent PDEδ degrader, was proven to possess good antitumor activity.

In summary, the HyT technology was identified as a feasible strategy for targeted degradation of PDEδ. HyT-based degrader **17c** exhibited a potent PDEδ binding affinity, PDEδ protein degradation activity, and antiproliferation activity, which represents a promising tool molecule or lead compound for further structural optimization and biological studies. This study also expands the application scope of the HyT approach and highlights the effectiveness of the HyT-based PDEδ degradation strategy in antitumor drug discovery.

■ ASSOCIATED CONTENT

Supporting Information

The Supporting Information is available free of charge at https://pubs.acs.org/doi/10.1021/acsmedchemlett.1c00670.

Additional information about the synthetic procedure, compound characterization and biological assays (PDF)

■ AUTHOR INFORMATION

Corresponding Authors

Guoqiang Dong − *School of Pharmacy, Second Military Medical University, Shanghai 200433, China*; Email: gdong@smmu.edu

Chunquan Sheng − *School of Pharmacy, Second Military Medical University, Shanghai 200433, China*; orcid.org/0000-0001-9489-804X; Email: cnshengcq@smmu.edu.cn

Authors

Menglu Guo − *School of Pharmacy, Second Military Medical University, Shanghai 200433, China*

Shipeng He − *Institute of Translational Medicine, Shanghai University, Shanghai 200444, China*

Junfei Cheng − *School of Pharmacy, Second Military Medical University, Shanghai 200433, China*

https://doi.org/10.1021/acsmedchemlett.1c00670
ACS Med. Chem. Lett. 2022, 13, 298−303

Yu Li − *School of Pharmacy, Second Military Medical University, Shanghai 200433, China*

Complete contact information is available at: https://pubs.acs.org/10.1021/acsmedchemlett.1c00670

Author Contributions

†M.G. and S.H. contributed equally to this work. G.D. and C.S. designed the experiments and revised the manuscript. M.G., S.H., and J.C. synthesized evodiamine borate derivatives and carried out the biological experiments. M.G., S.H., and Y.L. assisted with the biological experiments and in the preparation of the manuscript. All authors discussed the results and analyzed the data. All authors read and approved the final manuscript.

Funding

This work was supported by the National Key Research and Development Program of China (grant 2020YFA0509100 to C.S.), the National Natural Science Foundation of China (grants 21738002 and 82030105 to C.S., and 82003567 to S.H.), and Shanghai Rising-Star Program (20QA1411700 to G.D.)

Notes

The authors declare no competing financial interest.

■ ABBREVIATIONS

PPI, protein−protein interaction; HyT, hydrophobic tagging; KRAS, Kirsten rat sarcoma 2 viral oncogene homologue; PROTACs, proteolysis targeting chimeras; ERBB3, erythroblastosis oncogene B3; AR, androgen receptor; FP, fluorescence polarization; DC_{50}, concentration causing 50% protein degradation; CCK8, cell counting kit-8

■ REFERENCES

(1) Muzny, D. M.; Bainbridge, M. N.; Chang, K.; Dinh, H. H.; Drummond, J. A.; Fowler, G.; Kovar, C. L.; Lewis, L. R.; Morgan, M. B.; Newsham, I. F.; et al. Comprehensive molecular characterization of human colon and rectal cancer. *Nature* **2012**, *487*, 330−337.

(2) Akbani, R.; Akdemir, K. C.; Aksoy, B. A.; Albert, M.; Ally, A.; Amin, S. B.; Arachchi, H.; Arora, A.; Auman, J. T.; Ayala, B.; et al. Genomic classification of cutaneous melanoma. *Cell* **2015**, *161*, 1681−1696.

(3) Aguirre, A. J.; Hruban, R. H.; Raphael, B. J.; Canc Genome Atlas Res, N. Integrated genomic characterization of pancreatic ductal adenocarcinoma. *Cancer Cell* **2017**, *32*, 185−203.

(4) Malumbres, M.; Barbacid, M. Timeline - ras oncogenes: The first 30 years. *Nat. Rev. Cancer* **2003**, *3*, 459−465.

(5) Pylayeva-Gupta, Y.; Grabocka, E.; Bar-Sagi, D. Ras oncogenes: Weaving a tumorigenic web. *Nat. Rev. Cancer* **2011**, *11*, 761−774.

(6) Waters, A. M.; Der, C. J. Kras: The critical driver and therapeutic target for pancreatic cancer. *Cold Spring Harbor Perspect. Med.* **2018**, *8*, No. a031435.

(7) Cox, A. D.; Fesik, S. W.; Kimmelman, A. C.; Luo, J.; Der, C. J. Drugging the undruggable ras: Mission possible? *Nat. Rev. Drug Discovery* **2014**, *13*, 828−851.

(8) Kessler, D.; Gmachl, M.; Mantoulidis, A.; Martin, L. J.; Zoephel, A.; Mayer, M.; Gollner, A.; Covini, D.; Fischer, S.; Gerstberger, T.; et al. Drugging an undruggable pocket on kras. *Proc. Nat. Acad. Sci. U. S. A.* **2019**, *116*, 15823−15829.

(9) Zimmermann, G.; Papke, B.; Ismail, S.; Vartak, N.; Chandra, A.; Hoffmann, M.; Hahn, S. A.; Triola, G.; Wittinghofer, A.; Bastiaens, P. I. H.; Waldmann, H. Small molecule inhibition of the kras-pde delta interaction impairs oncogenic kras signalling. *Nature* **2013**, *497*, 638−642.

(10) Spiegel, J.; Cromm, P. M.; Zimmermann, G.; Grossmann, T. N.; Waldmann, H. Small-molecule modulation of ras signaling. *Nat. Chem. Bio.* **2014**, *10*, 613−622.

(11) Chen, F.; Alphonse, M. P.; Liu, Y.; Liu, Q. Targeting mutant kras for anticancer therapy. *Curr. Top. Med. Chem.* **2019**, *19*, 2098−2113.

(12) Liu, P.; Wang, Y.; Li, X. Targeting the untargetable kras in cancer therapy. *Acta Pharm. Sin. B* **2019**, *9*, 871−879.

(13) Klein, C. H.; Truxius, D. C.; Vogel, H. A.; Harizanova, J.; Murarka, S.; Martin-Gago, P.; Bastiaens, P. I. H. Pde delta inhibition impedes the proliferation and survival of human colorectal cancer cell lines harboring oncogenic kras. *Int. J. Cancer* **2019**, *144*, 767−776.

(14) Martin-Gago, P.; Fansa, E. K.; Wittinghofer, A.; Waldmann, H. Structure-based development of pde delta inhibitors. *Bio. Chem.* **2017**, *398*, 535−545.

(15) Papke, B.; Murarka, S.; Vogel, H. A.; Martin-Gago, P.; Kovacevic, M.; Truxius, D. C.; Fansa, E. K.; Ismail, S.; Zimmermann, G.; Heinelt, K.; et al. Identification of pyrazolopyridazinones as pded inhibitors. *Nat. Commun.* **2016**, *7*, 11360.

(16) Murarka, S.; Martin-Gago, P.; Schultz-Fademrecht, C.; Al Saabi, A.; Baumann, M.; Fansa, E. K.; Ismail, S.; Nussbaumer, P.; Wittinghofer, A.; Waldmann, H. Development of pyridazinone chemotypes targeting the pde prenyl binding site. *Chem.—Eur. J.* **2017**, *23*, 6083−6093.

(17) Zimmermann, G.; Schultz-Fademrecht, C.; Kuechler, P.; Murarka, S.; Ismail, S.; Triola, G.; Nussbaumer, P.; Wittinghofer, A.; Waldmann, H. Structure guided design and kinetic analysis of highly potent benzimidazole inhibitors targeting the pde delta prenyl binding site. *J. Med. Chem.* **2014**, *57*, 5435−5448.

(18) Martin-Gago, P.; Fansa, E. K.; Klein, C. H.; Murarka, S.; Janning, P.; Schuermann, M.; Metz, M.; Ismail, S.; Schultz-Fademrecht, C.; Baumann, M.; Bastiaens, P. I. H.; Wittinghofer, A.; Waldmann, H. A pde6 delta-kras inhibitor chemotype with up to seven h-bonds and picomolar affinity that prevents efficient inhibitor release by arl2. *Angew. Chem., Int. Ed.* **2017**, *56*, 2423−2428.

(19) Chen, L.; Zhuang, C.; Lu, J.; Jiang, Y.; Sheng, C. Discovery of novel kras-pde delta inhibitors by fragment-based drug design. *J. Med. Chem.* **2018**, *61*, 2604−2610.

(20) Jiang, Y.; Zhuang, C.; Chen, L.; Lu, J.; Dong, G.; Miao, Z.; Zhang, W.; Li, J.; Sheng, C. Structural biology-inspired discovery of novel kras-pde delta inhibitors. *J. Med. Chem.* **2017**, *60*, 9400−9406.

(21) Neklesa, T. K.; Crews, C. M. Chemical biology greasy tags for protein removal. *Nature* **2012**, *487*, 308−309.

(22) Wang, Y.; Jiang, X.; Feng, F.; Liu, W.; Sun, H. Degradation of proteins by protacs and other strategies. *Acta Pharm. Sin. B* **2020**, *10*, 207−238.

(23) Lai, A. C.; Crews, C. M. Induced protein degradation: An emerging drug discovery paradigm. *Nat. Rev. Drug Discovery* **2017**, *16*, 101−114.

(24) Neklesa, T. K.; Tae, H. S.; Schneekloth, A. R.; Stulberg, M. J.; Corson, T. W.; Sundberg, T. B.; Raina, K.; Holley, S. A.; Crews, C. M. Small-molecule hydrophobic tagging-induced degradation of halotag fusion proteins. *Nat. Chem. Bio.* **2011**, *7*, 538−543.

(25) Xie, T.; Lim, S. M.; Westover, K. D.; Dodge, M. E.; Ercan, D.; Ficarro, S. B.; Udayakumar, D.; Gurbani, D.; Tae, H. S.; Riddle, S. M.; Sim, T.; Marto, J. A.; Jaenne, P. A.; Crews, C. M.; Gray, N. S. Pharmacological targeting of the pseudokinase her3. *Nat. Chem. Bio.* **2014**, *10*, 1006−1012.

(26) Gustafson, J. L.; Neklesa, T. K.; Cox, C. S.; Roth, A. G.; Buckley, D. L.; Tae, H. S.; Sundberg, T. B.; Stagg, D. B.; Hines, J.; McDonnell, D. P.; Norris, J. D.; Crews, C. M. Small-molecule-mediated degradation of the androgen receptor through hydrophobic tagging. *Angew. Chem., Int. Ed.* **2015**, *54*, 9659−9662.

(27) Cheng, J.; Li, Y.; Wang, X.; Dong, G.; Sheng, C. Discovery of novel pdeδ degraders for the treatment of kras mutant colorectal cancer. *J. Med. Chem.* **2020**, *63*, 7892−7905.